Desalination and Water Treatment
www.deswater.com

doi: 10.5004/dwt.2017.21103

84 (2017) 190–198
July

Preparation, characterization and catalytic performance of paper mill sludge and municipal wastewater treatment sludge-based catalysts for Fenton-like oxidation of Rhodamine B

Meifang Hou[a], Yuanyuan Guo[a,b], Xiaoyang Chen[b,]*, Min Xiao[c], Chunlai Hong[b], Yanlai Yao[b], Fengxiang Zhu[b], Weiping Wang[b]

[a]*Shanghai Institute of Technology, Shanghai 201418, China*
[b]*Institute of Environmental Resource and Soil Fertilizer, Zhejiang Academy of Agricultural Sciences, Hangzhou 310021, China, Tel. +86-571-86404079; Fax: +86-571-86404208; email: xiaoyangchen@aliyun.com (X. Chen)*
[c]*Shenyang University, Shenyang 110044, China*

Received 28 March 2017; Accepted 30 June 2017

ABSTRACT

In this study, sludge-derived Fenton-like catalysts, namely potentially low cost, were successfully synthesized through a unique and original method, which was used to oxidative degradate Rhodamine B (RhB) as heterogeneous Fenton-like Fe/C catalysts. Two types of sludge sources were used as sludge-derived support carbon: paper mill sludge and municipal wastewater treatment sludge. This unique preparation method converted pyrolyzed sludge into a porous carbon-based carrier material by chemical activation and then used an iron loading impregnation method to synthesize the Fenton-like Fe/C catalyst. The prepared two types of catalysts including paper mill sludge-derived char-supported iron catalyst and municipal sewage sludge-derived char-supported iron catalyst were characterized in terms of Fourier transform infrared spectroscopy, X-ray diffraction, scanning electron microscopy and N_2-adsorption/desorption. Compared with sludge-derived Fe/C catalyst without activation, both the PMSC-Fe and the MSSC-Fe catalyst exhibited much better catalytic performance in degrading RhB. Both PMSC-Fe and MSSC-Fe exhibited excellent catalytic stability and almost seldom Fe-ion leaching. A correlation could be found between surface area and RhB degradation, suggesting that surface area of the catalyst is an important factor for the catalytic performance. Two different sources of sludge also showed discrepancy in catalytic performance of RhB degradation, which is perhaps due to the different properties of the initial sewage sludge. The catalyst of PMSC-Fe and MSSC-Fe both has an excellent long-term stability. Possible degradation mechanism of RhB induced by sludge-derived Fe-C/H_2O_2 system is proposed.

Keywords: Heterogeneous catalyst; Sewage sludge-based catalyst; Fenton like; Rhodamine B

1. Introduction

As the rate of municipal and industrial wastewater treatment increases, large sludge quantities are generated in the treatment process. This increasing amount of sludge has become an issue of particular concern, and sewage sludge disposal is an important environmental problem [1,2]. Traditional methods of sewage sludge disposal, such as ocean dumpling, landfill, incineration and composting land application, may have potential environmental risks to soil, ground water and air [2–4]. Because some of these traditional disposal options are progressively becoming restricted, it is necessary to explore novel and value-added methods to maximize the recovery of useful materials and minimize the residue from sewage sludge [2,5].

---

* Corresponding author.

1944-3994/1944-3986 © 2017 Desalination Publications. All rights reserved.

In this context, the high costs of adsorbent and catalyst manufacture have prompted a growing interest into the utilization of sewage sludge and other waste precursors to produce low cost forms of these materials [6,7]. In fact, sewage sludge, especially paper mill sludge and municipal wastewater treatment sludge, is carbonaceous in nature [8,9]. Hence, it has the potential to be converted into porous-activated carbon under controlled conditions or with some chemical treatments. The process of pyrolyzing sludge into sludge-derived biochar is effective in reducing sludge volume and produces useful end products [10–14]. At the same time, the process destroys most pathogenic organisms and stabilizes most toxic heavy metals. Previous studies on sludge-derived carbon mainly focused on sludge-based adsorbent, where sludge-based carbon had been used to adsorb different dyes [15], heavy metals [16], organic pollutants [17] and odor gases [18]. Recently, sewage sludge-derived material was reported for catalytic wet air oxidation of phenolic compounds [17], a catalyst for ozonation oxidation [9], and as the support of TiO_2 photocatalyst [19–21]. Most recently, many studies showed that sewage sludge-derived mesoporous material is also an efficient and stable heterogeneous catalyst for Fenton-like reactions [22,23]. Therefore, sewage sludge-derived material can be used as a heterogeneous catalyst for Fenton-like reactions to achieve high catalytic activity and long-term stability. For example, the municipal wastewater treatment sludge can be directly synthesized into Fenton catalyst, which has a high catalytic activity in degradation of Acid Orange II, and the efficiency achieves at 98% within 30 min [24]. This kind of sludge carbon material also shows high catalytic in 1-dizao-2-naphthol-4-sulfonic acid, and its removal efficiency can reach 96.6% after 260 min Fenton-like treatment [19]. The paper mill sludge can be synthesized into Fenton-like catalyst, which has a high catalytic in methylene blue, and the efficiency achieves at 95% within 40 min [25,26]. According to these studies, the sources of sewage sludge have important effects on the efficiency of the synthesized materials.

The Fenton reaction is an effective process that degrades recalcitrant organic pollutants using strong, relatively non-selective hydroxyl radicals (·OH) [27,28]. However, some drawbacks restrict widespread, industrial-scale application of homogeneous Fenton reactions, such as pH limitations and recycling difficulty. This has led to the development of a heterogeneous catalyst for the Fenton system [29–31]. Heterogeneous catalysts are noncorrosive, environmentally benign and easy to separate from treated wastewater. They might be the most promising catalysts for hazardous waste remediation and water disinfection. Many studies have been performed, and various supports have been employed to prepare heterogeneous catalysts for the Fenton process [32–34]. However, heterogeneous catalysts also encounter problems, such as high Fe leaching and poor stability. Therefore, a cost-effective heterogeneous catalyst with high catalytic activity and good support with long-term stability is essential to elevate catalytic efficiency and application.

In our study, two types of sludge including paper mill sludge and municipal wastewater treatment sludge were selected as sludge-derived support carbon. For the synthesis process of Fe/C catalysts, the unique two-step synthesis method was chosen, which includes activation of sludge-derived carbon support and then iron loading on the sludge-derived carbon. The catalytic performance of the synthesized paper mill sludge-derived catalysts and municipal sewage sludge-derived catalysts during Fenton system were investigated using Rhodamine B (RhB), which is present in most textile industrial wastewaters and harmful to humans on contact and toxic to aquatic organisms. To our knowledge, little information on the comparative study of these two different sources sludge-derived Fe/C catalyst on heterogeneous Fenton-like degradation of RhB is available from previous studies. Hence, this study not only intends to provide an environmentally friendly sewage reuse method but also study the discrepancy of the two types of carbon-rich sludge (paper mill sludge and municipal wastewater treatment sludge) as the Fenton-like catalyst support.

2. Materials and methods

2.1. Materials

Paper mill sludge was obtained in November from the Chun Nan papermaking plant in Fu Yang, Hangzhou, China. Municipal sewage sludge was obtained in November from the Fu Yang municipal wastewater treatment plant in Hangzhou, China. Both types of sludge were dried at 105°C to a constant weight, subsequently ground and sifted through an 80-mesh sieve, and then stored in a desiccator at room temperature.

All reagents, including $ZnCl_2$, H_2SO_4, $Ca(OH)_2$, $FeSO_4$, RhB and H_2O_2 (30%, w/v) were analytical reagent unless otherwise stated which was purchased from Sinopharm Chemical Reagent Company, Shanghai, China. All solutions were prepared with water obtained from a water purification system (Milli-Q Advantage A10 Water Purification System).

2.2. Preparation of catalysts

The sewage sludge-derived char supported iron oxide catalyst was prepared in two steps: activation of sewage sludge-derived char and loading of iron oxide. For paper mill sludge, 5 mol/L $ZnCl_2$ and 40% H_2SO_4 as activating agents were added to 6 g of dried sludge. The $ZnCl_2$-to-H_2SO_4 ratio was 3:1, and the solid-to-liquid ratio was 1:2.5 (g/mL). For municipal sewage sludge, 5 mol/L $ZnCl_2$ and 4 wt% $Ca(OH)_2$ as activating agents were added to 6 g of dried sludge. The dried sludge-to-$ZnCl_2$ ratio was 1:1 (g/mL). During the activation process, contact was maintained between the liquid and solid phases using mechanical shaking at a constant rate of 180 rpm for 1 h at 20°C. Then, the materials were dried at 105°C for 5 h. Subsequently, the dried solids were pyrolyzed in a horizontal tube furnace at 550°C for 1 h with a heating rate of 20°C/min and a nitrogen flow of 0.1 m^3/h. The pyrolyzed samples were rinsed with 3 mol/L hydrochloric acid to remove other inorganic matter, washed with 70°C deionized water several times until the pH became neutral, cleaned in a 50 W ultrasonic washer for 10 min, dried at 80°C overnight and ground to less than 200-mesh.

For the loading process, 10 g of dried sewage sludge-derived char was added to 30 mL of 0.1 mol/L $FeSO_4·7H_2O$ solution, dipped for 1 h, stirred for 24 h, and dried at 105°C for 12 h. Finally, the dried char was pyrolyzed in a horizontal tube furnace at 350°C for 2 h with a heating rate of 20°C/min and a nitrogen flow of 0.1 m^3/h. The obtained samples were rinsed with deionized water until the electrical conductivity remained stable and then dried at 80°C.

To explore the influence of different factors on catalyst loading, the $FeSO_4$ concentration and pyrolysis temperature were set as variables in the pyrolysis experiment. $FeSO_4$ concentrations of 0.1, 0.25 and 0.5 mol/L were selected to investigate the effect of concentration on catalyst performance. We selected pyrolysis temperatures of 350°C, 450°C and 550°C to explore the effect of pyrolysis temperature on catalyst performance. In addition, we compared activated catalysts with catalysts obtained by loading directly without activation.

2.3. Characterization of catalysts

The functional groups of as-synthesized catalysts were detected by Fourier transform infrared (FTIR) spectroscopy (Thermo Nicolet 380, USA). The catalyst crystal structures were characterized using X-ray diffraction (XRD; Bruker D8 Advance, Germany). The surface area was determined using the Brunauer–Emmett–Teller (BET) method (Quantachrome nova 2000e, USA). The surface morphology was observed using scanning electron microscopy (SEM; Hitachi S-3400N, Japan). The leaching concentration of Fe in the solution was measured by inductively coupled plasma optical emission spectrometry (ICP-OES; Agilent 720, USA). The chemical composition of each element present was analyzed via automatic element analyzer (Euro Vector EA3000, Italy).

2.4. RhB degradation

All batch experiments were carried out at room temperature in a glass conical beaker (250 mL) with a stopper shaker on a magnetic stirrer at an equivalent stirring velocity. During the reaction, 0.05 g of catalyst was added to 150 mL of 50 mg/L RhB solution. The solution pH was adjusted to 4.0 ± 0.1 with H_2SO_4. The suspension was stirred in the dark for 1 h to disperse the catalyst and achieve adsorption/desorption equilibrium. After the first sample was taken, the degradation reaction was initiated by adding 1 mL of 3% H_2O_2 to the reaction solution. At given time intervals during the reaction, solution samples were taken and centrifuged to immediately remove any catalyst particles.

The pH of the RhB solution was measured with a PHS-3C pH meter (Rex Instrument Factory, Shanghai, China). RhB concentration was analyzed using a UV–Vis spectrophotometer (UV-3150, Shimadzu) with maximum absorbance at 484 nm.

3. Results and discussion

3.1. Characterization of the catalysts

The four prepared catalysts paper mill sludge-derived char-supported iron catalyst through activation (PMSC-Fe), municipal sewage sludge-derived char-supported iron catalyst through activation (MSSC-Fe), paper mill sludge-derived catalyst by direct loading without activation (PMS-Fe) and municipal sewage sludge by direct loading without activation (MSS-Fe) were characterized. The preparation conditions were as follows: the calcination temperature was 350°C and the concentration of $FeSO_4$ was 0.1 mol/L.

FTIR spectra were used to determine the functional groups and chemical bonds on the catalyst surfaces and the results were shown in Fig. 1. As shown in Fig. 1, the broad band at approximately 3,400 cm^{-1} corresponded to the O–H stretching vibration of hydroxyl functional groups, including hydrogen bonding. The band at approximately 1,630 cm^{-1} was ascribed to the C=O stretching vibration of carbonyl groups [35]. A weak peak at 1,385 cm^{-1} was attributed to the presence of C–H, whose stretching vibration appeared to overlap with the 3,400 cm^{-1} band of –OH [36]. The broad band at 1,035 cm^{-1} was primarily attributed to the C–O stretching vibration. The broad, high-intensity band at 1,080 cm^{-1} was attributed to asymmetric Si–O–Si stretching vibrations, while the Si–O–Si symmetrical stretching gave rise to the peak at 795 cm^{-1}. The peaks at approximately 690 and 470 cm^{-1} corresponded to the characteristic symmetric stretching vibration and bending vibration of Si–O–Fe [20]. In addition, some different peaks were found in the PMSC-Fe curve, such as the peak at 1,430 cm^{-1}, which was assigned to $–NO_2$ [36], and the peak at 873 cm^{-1}, which was assigned to Si–O [37]. These results clearly indicated formation of chemical bonds between inorganic compounds in the sewage sludge and the loaded Fe compound in the catalyst. Compared with PMS-Fe and MSS-Fe, PMSC-Fe and MSSC-Fe with chemical activation had obvious Si–O–Fe, which proved that catalyst with activation was more stable. Determining the functional groups and chemical bonds on the catalyst surfaces will provide important contributions to analyze the reaction mechanism of the catalyst.

As shown in Fig. 2, XRD patterns of four prepared sludge-derived Fe/C catalyst were illustrated. All the materials displayed two primary diffraction peaks at 2θ = 21.0° and 26.7° except for PMS-Fe, which corresponded to typical SiO_2 (quartz) crystallite structures [20]. PMS-Fe displayed a primary diffraction peak at 2θ = 29.4°, which corresponded to typical $CaCO_3$ (calcite) [26]. PMSC-Fe displayed four primary diffraction peaks at 2θ = 28.8°, 30.8°, 47.8° and 56.7°, corresponding to typical ZnS, which might be due to the presence of the activation agents $ZnCl_2$ and H_2SO_4 during the activation process. PMSC-Fe, PMS-Fe and MSSC-Fe displayed diffraction peaks at 2θ = 33.0°, 36.7° and 39.7°, which

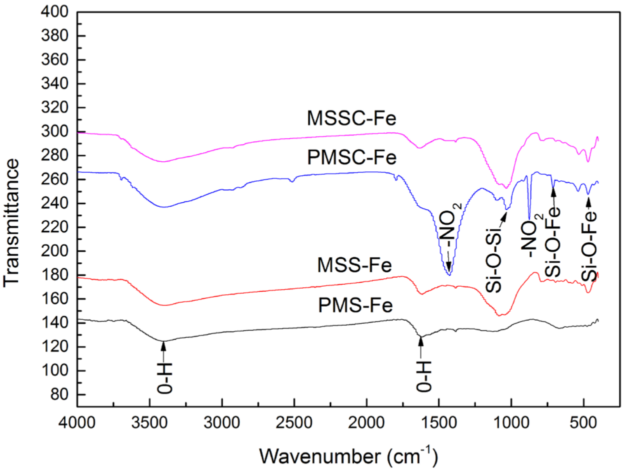

Fig. 1. FTIR spectra of the catalysts.

were assigned to the (104), (110) and (113) reflections of α-Fe_2O_3 (hematite) (JCPDS, File No. 840306) [26]. Thus, these results suggest that PMSC-Fe primarily consisted of SiO_2, α-Fe_2O_3 and ZnS crystallites; PMS-Fe primarily consisted of α-Fe_2O_3 and $CaCO_3$ crystallites; MSSC-Fe primarily consisted of SiO_2 and α-Fe_2O_3 crystallites; and MSS-Fe primarily consisted of SiO_2 crystallites. The α-Fe_2O_3 crystallites played a major role in Fenton-like catalytic reactions.

Table 2 provides the BET surface areas (S_{BET}), micropore areas (S_{micro}), external surface areas (including mesopore and macropore areas, S_{ext}), micropore volumes (V_{micro}), total pore diameters (V_t) and average pore diameters (D_{ap}) of the catalysts. Compared with PMS-Fe (S_{BET}, 31.13 m²/g) and MSS-Fe (S_{BET}, 26.74 m²/g), the catalysts with chemical activation, namely, PMSC-Fe (S_{BET}, 418.45 m²/g) and MSSC-Fe (S_{BET}, 351.99 m²/g), had remarkably high BET surface areas. PMSC-Fe had a larger BET surface than MSSC-Fe perhaps mainly because paper mill sludge had higher carbon content than municipal sewage sludge (Table 1). Besides, paper mill sludge had more fine cellulosic fibers, fibers too short to be retained on fiber screens and paper machines, and inorganic material [25]. During carbonization, organic carbon materials in sludge were carbonized and thus left the open space previously occupied. This could also lead to larger surface areas. Catalysts with activation (PMSC-Fe and MSSC-Fe) had larger micropore areas, while the micropore areas of PMS-Fe and MSS-Fe were zero. PMSC-Fe and MSSC-Fe had a higher proportion of micropores and mesopores, whereas PMS-Fe and MSS-Fe contained more mesopores and macropores. In order to further study the effect of calcination temperature on catalyst, the BET surface areas, micropore areas, external surface areas of PMSC-Fe at different calcination temperatures (350°C, 450°C and 550°C) were determined. The results showed that the BET surface areas, micropore areas, external surface areas of PMSC-Fe catalyst decreased with the increase of calcination temperature. This might be because of that high calcination temperature destroyed the porous structure of the sludge carbon carrier. Besides, from the economic point of view, low calcination temperature had low energy consumption.

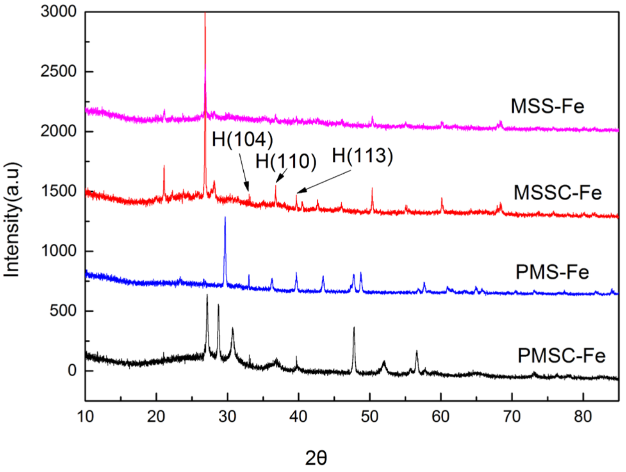

Fig. 2. XRD spectra of the catalysts.

Table 1
Physicochemical properties of synthesized sewage-derived catalysts and sewage sludge

Sample	N%	C%	S%	Fe (%)	Si (mg/g)
PMSC-Fe	2.850	29.775	2.422	3.377	0.191
MSSC-Fe	2.139	17.611	0	2.549	0.323
PMS-Fe	1.818	19.809	0	6.180	0.278
MSS-Fe	1.765	11.537	0	6.270	0.219
PMS	3.093	25.752	0	2.736	0.295
MSS	3.282	18.678	0	3.522	0.239
PMSC-Fe-0.1	–	–	–	3.107	0.272
PMSC-Fe-0.25	–	–	–	5.886	0.162
PMSC-Fe-0.5	–	–	–	10.104	0.205

SEM was employed to observe the surface physical morphology of sludge-derived activated carbon catalysts, as shown in Fig. 3. As seen in the micrographs, PMSC-Fe and MSSC-Fe contain lots of well-developed pores with different shapes, resulting from evaporation of the $ZnCl_2$, H_2SO_4 and $Ca(OH)_2$ chemical reagents during carbonization, leaving open the space previously occupied by the reagents. PMS-Fe and MSS-Fe exhibited coarse and nonporous surfaces due to the evaporation of H_2O and decomposition of organic sludge molecules during calcination. Additionally, as shown in Table 1, PMS-Fe and MSS-Fe had a higher Fe content than PMSC-Fe and MSSC-Fe. The presence of more iron might block pore development in porous material. Compared with municipal sewage sludge-derived catalysts, paper mill sludge-derived catalysts exhibited a higher number of pores at a higher density, potentially due to the composition of paper mill sludge, which contained more fine cellulosic fibers and inorganic materials.

Table 2
Characteristics of the porous structure of catalyst

Catalyst	S_{BET} (m²/g)	S_{micro} (m²/g)	S_{ext} (m²/g)	V_{micro} (cm³/g)	V_t (cm³/g)	D_{ap} (nm)
PMSC-Fe (350°C)	418.45	219.92	198.54	0.094	0.31	2.67
PMS-Fe (350°C)	31.13	0	31.13	0	0.058	7.44
MSSC-Fe (350°C)	351.99	215.53	136.47	0.090	0.25	2.89
MSS-Fe (350°C)	26.74	0	26.74	0	0.078	11.69
PMSC-Fe (450°C)	409.54	159.7	249.8	0.037	0.36	3.59
PMSC-Fe (550°C)	369.66	128.3	241.3	0.054	0.31	3.40

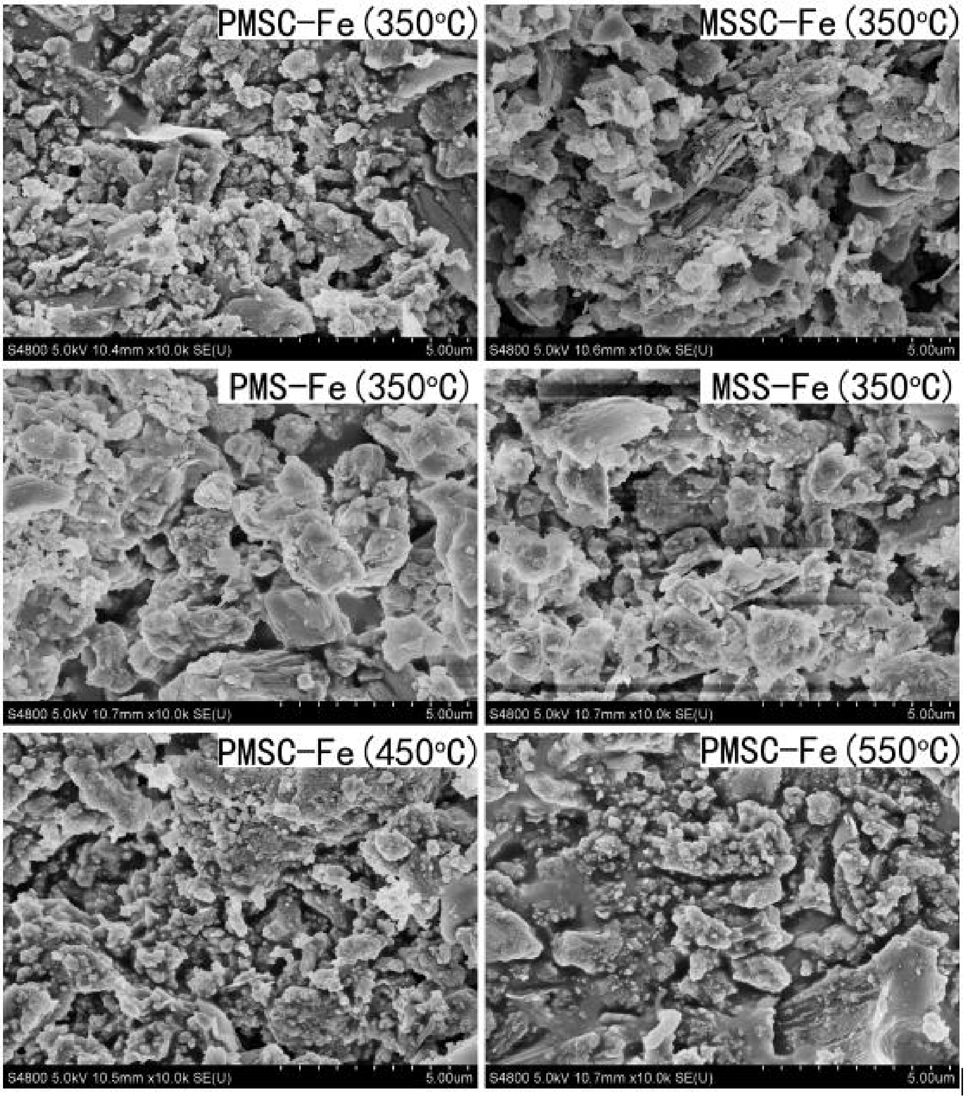

Fig. 3. SEM images of the catalysts.

The microstructure of the prepared PMSC-Fe catalyst with increasing calcinations temperature is also presented in Fig. 4. At 350°C and 450°C, the catalyst particle was distributed uniformly, and the catalyst has obvious pore structure. As the calcinations temperature approaches to 550°C, part of the catalyst became conglomeration and appeared sheet structure, which would cause the BET surface areas of catalyst decreased (Table 2). Therefore, calcinations temperature might be one of the factors which influenced the structure and catalytic activity of the sludge-derived catalysts.

3.2. RhB degradation

Fenton-like catalytic performance of different systems was assessed in terms of RhB degradation efficiency and the results were shown in Fig. 4. RhB was scarcely degraded under H_2O_2 alone, perhaps because H_2O_2 was stable at room temperature and the chemical reaction was relatively slow in the absence of catalysts. No obvious RhB degradation was detected in the

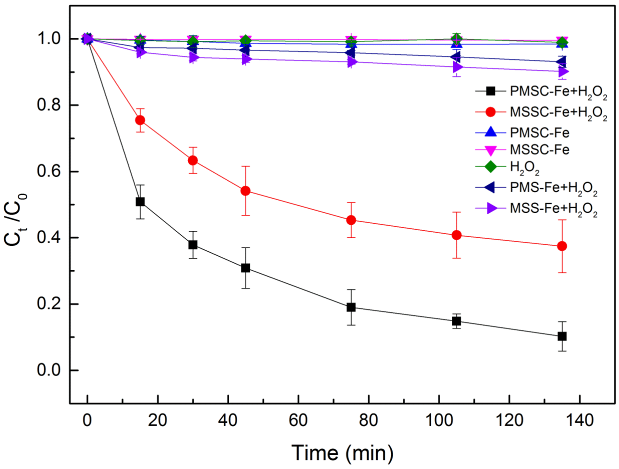

Fig. 4. RhB degradation under different systems (conditions: [RhB] = 50 mg/L, [Catalysts] = 0.33 g/L, $[H_2O_2]$ = 6 mmol/L, pH = 4).

presence of PMSC-Fe and MSSC-Fe. This may be because the catalysts maintained adsorption–desorption equilibrium with RhB from the preceding 60 min of stirring, which can eliminate the effect of catalyst adsorption during the degradation process. When PMSC-Fe was added to the solution with H_2O_2, the degradation rate reached 90%, and the degradation rate of MSSC-Fe was 43%. The catalytic activity of the paper mill sludge-derived catalyst was clearly higher than that of the municipal sewage sludge-derived catalyst. This is because the paper mill sludge had fine cellulosic fiber and more inorganic material. In the pyrolysis process, cellulosic fiber and inorganic materials evaporated with N_2 and left more holes. This process increased the surface area of PMSC-Fe and thus increased the catalytic activity. As shown in Table 2, the BET surface areas of PMSC-Fe and MSSC-Fe were 418.45 and 351.99 m^2/g, respectively. For the same reason, the degradation rate of PMS-Fe and MSS-Fe was only approximately 10% because PMS-Fe and MSS-Fe were synthetized without activation. This led to very low BET surface areas. The BET surface areas of PMS-Fe and MSS-Fe were 31.13 and 26.74 m^2/g, and the micropore areas of PMS-Fe and MSS-Fe were zero (Table 2). A high surface area increased the surface active sites of the catalysts and enhanced the catalyst degradation ability.

Fig. 5 shows the effect of $FeSO_4$ concentration of two kinds of sewage sludge-derived catalysts during the loading process on RhB degradation in catalytic experimentation. For paper mill sludge-derived catalyst, the RhB best degradation rate was 70% when the $FeSO_4$ loading concentration was 0.1 mol/L. The degradation rate was 52% and 28% when the $FeSO_4$ loading concentration was 0.25 and 0.5 mol/L, respectively. For municipal sewage sludge-derived catalyst, the RhB best degradation rate was 47% when the $FeSO_4$ loading concentration was 0.1 and 0.25 mol/L, the removal rate was only 18% when the $FeSO_4$ concentration was 0.5 mol/L. These results might be due to an increase in material density and blocking of pores within the mesoporous material as Fe incorporation (α-Fe_2O_3) increased. As shown in Table 1, increasing the loading concentration of $FeSO_4$, increased the iron content of the catalyst. This reduced the surface active sites, and the catalyst degradation ability decreased. Compared with municipal sewage sludge-derived catalyst, paper mill sludge-derived catalyst displayed higher catalytic activity at each $FeSO_4$ concentration. This result further confirmed that paper mill sludge-derived catalyst had a higher catalytic activity than municipal sewage sludge-derived catalyst.

A comparison of RhB degradation of paper mill sludge-derived catalyst and municipal sewage sludge-derived catalyst under different calcination temperatures after Fe loading is shown in Fig. 6. For paper mill sludge-derived catalyst, the best degradation rate of RhB was 90% when the calcination temperature was 350°C, while the municipal sewage sludge-derived catalyst was 60%. The degradation rate of RhB of paper mill sludge-derived catalyst was approximately 66% when the calcination temperatures were 450°C and 550°C, while the municipal sewage sludge-derived catalyst was 60% and 40%, respectively. These results might be due to the second calcination after Fe loading destroyed the mesoporous structure of the catalyst surface and catalyst became conglomeration as shown in Fig. 3. The higher the calcination temperature, the more serious is the damage to the mesoporous structure of the catalyst surface. The measured BET surface areas reinforce this hypothesis. The BET surface areas of PMSC-350, PMSC-450 and PMSC-550 were 418.45, 409.54 and 369.66 m^2/g, respectively. Destruction of the mesoporous structure reduced the surface active sites and decreased the catalyst degradation ability.

3.3. Mechanism

To illustrate the transformation of RhB structural and molecular features in the degradation process, UV–Vis spectral changes over time were observed (Fig. 7). As shown, the absorption spectrum of RhB in aqueous solution was mainly characterized by two bands. The visible absorbance band at 554 nm, which is used to monitor residual RhB, corresponds RhB degradation because of the conjugated structure of C=O groups. The UV absorbance at 259 nm corresponds to the existence of aromatic rings in RhB [38]; the intensity reflected

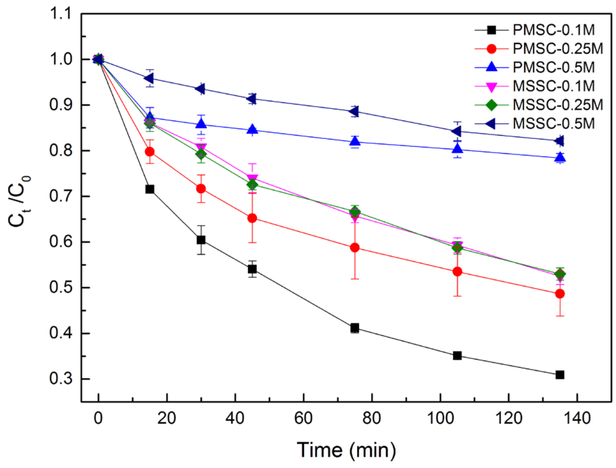

Fig. 5. Effect of the $FeSO_4$ concentration in PMSC and MSSC on RhB degradation (conditions: [RhB] = 50 mg/L, [PMSC-Fe] = 0.33 g/L, $[H_2O_2]$ = 6 mmol/L, pH = 4).

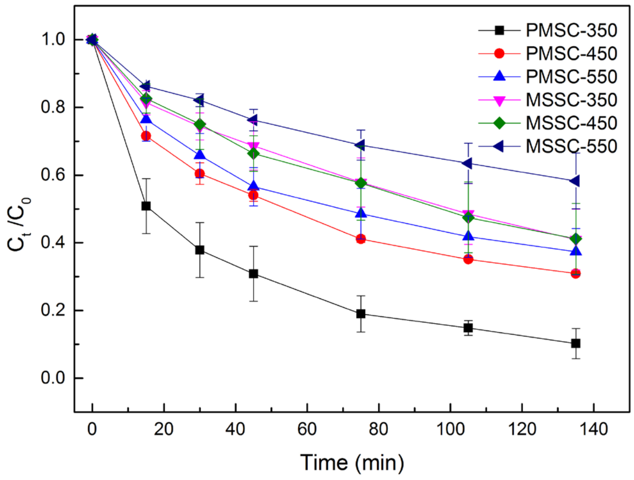

Fig. 6. Effect of calcination temperature in PMSC-Fe and MSSC-Fe on RhB degradation (conditions: [RhB] = 50 mg/L, [PMSC-Fe] = 0.33 g/L, $[H_2O_2]$ = 6 mmol/L, pH = 4).

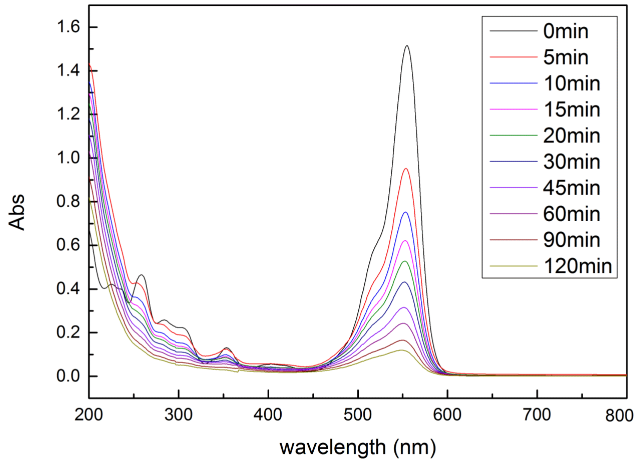

Fig. 7. UV–Vis spectra of RhB solution at different times using PMSC-Fe as the catalyst.

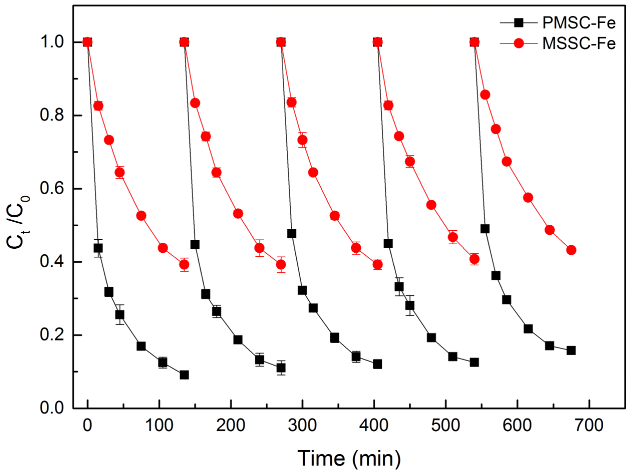

Fig. 8. Cyclic degradation in RhB degradation.

its concentration in solution. The disappearance of the visible band with reaction time correlated with RhB degradation. It has been reported that RhB degrades through two competitive pathways: *N*-demethylation or cleavage of the chromophore structure [39]. The signal at 554 nm diminished rapidly within the first 15 min and then slowly until 60 min, following the degradation of the RhB solution. The decrease in absorbance at 259 nm indicated that the aromatic moiety was degraded to smaller aliphatic compounds and eventually to CO_2 and H_2O.

Based on the above results, PMSC-Fe showed efficient RhB Fenton-like degradation ability. However, it is not clear whether the high RhB degradation rate can be attributed to the presence of PMSC-Fe or ions in solution leaching from PMSC-Fe under acidic condition. To investigate the contribution of homogeneous catalytic reaction, the degradation of RhB by leached Fe ions was investigated. The leached Fe-ion concentration was determined by ICP after 135 min. The leached Fe-ion concentrations of PMSC-Fe, MSSC-Fe, PMS-Fe and MSS-Fe were 0, 0.0262, 0.0054 and 0.0042 mg/L, respectively. The catalysts exhibited very low Fe-ion concentrations because of the formation of a chemical bond (Fe–O–Si) between the loaded Fe compound and SiO_2, which guarantees catalyst stability. Because almost zero iron leaching was observed, it can be deduced that the main contribution was from the heterogeneous Fenton-like reaction and not the homogeneous reaction.

In addition, we propose a possible mechanism for the heterogeneous catalyst for the RhB degradation described by Eqs. (1)–(5). First, RhB was adsorbed on the catalyst surfaces. Then, H_2O_2 adsorbed on carbon by hydrogen bonds with oxygen in siloxane bridges (Eq. (1)), leading to a higher concentration of H_2O_2 on the catalyst surfaces than in the bulk solution, facilitating the Fenton-like reaction. Subsequently, the redox cycle of Fe^{3+}/Fe^{2+} on the catalyst surface was initiated by the addition of H_2O_2 (Eqs. (2) and (3)) [32]. Several studies have suggested that the carbon material is responsible for the decomposition of the H_2O_2 into $^{\bullet}OH$ which are powerful oxidants (Eq. (4)) [40–42]. Finally, adsorbed RhB molecules were decomposed into CO_2 and H_2O by the generated $^{\bullet}OH$ radicals on the catalyst surfaces while the catalyst itself was restored to the original state (Eq. (5)) [43].

$$H_2O_2 + \equiv\text{Carbon} \rightarrow \equiv\text{Carbon} + {}^{\bullet}H_2O_2 \tag{1}$$

$$\equiv Fe^{3+} + H_2O_2 \rightarrow \equiv Fe^{2+} + H^+ + {}^{\bullet}OOH \tag{2}$$

$$\equiv Fe^{2+} + H_2O_2 \rightarrow \equiv Fe^{3+} + OH^- + {}^{\bullet}OH \tag{3}$$

$$\text{Carbon} + H_2O_2 \rightarrow \equiv\text{Carbon}^+ + OH^- + {}^{\bullet}OH \tag{4}$$

$$\text{RhB} + {}^{\bullet}OH \rightarrow CO_2 + H_2O \tag{5}$$

where ≡ represents the surface of the catalyst.

3.4. Reusability and stability of catalysts

To test the stability and recyclability of PMSC-Fe, five recycling runs of PMSC-Fe and MSSC-Fe were carried out as shown in Fig. 8. No obvious deactivation of the PMSC-Fe catalyst in the five repetitions was observed when compared with the first cycle, indicating its excellent long-term stability. Based on the negligible Fe leaching from the PMSC-Fe catalyst during the degradation reaction, the excellent catalytic stability can be attributed to the catalyst's structure. All these results indicate that the catalyst has excellent stability and great potential application value.

4. Conclusions

In summary, we synthesized two types of sewage sludge-derived mesoporous catalytic materials, PMSC-Fe and MSSC-Fe, via a two-step method and demonstrated their efficiency and stability as heterogeneous catalysts for Fenton-like reactions. The XRD results showed PMSC-Fe and MSSC-Fe catalysts mainly contained α-Fe_2O_3, which played a major role in Fenton-like catalytic reactions. Compared with sewage sludge-derived Fe/C without activation, PMSC-Fe and MSSC-Fe have extremely high BET surface areas, which plays an important factor for the catalytic performance.

The experimental results showed that the optimum synthesis conditions of catalysts were 0.1 mol/L $FeSO_4$ impregnation concentration and 350°C calcination temperatures. The catalytic activity of PMSC-Fe was better than MSSC-Fe perhaps due to the different properties of the initial sewage sludge. Our results also demonstrated that the catalyst exhibited negligible iron leaching and high catalytic ability after five reaction cycles. The results presented in this paper offer new opportunities for environmentally friendly reuse of paper mill sludge and municipal sewage sludge and provide a method for synthesizing a mesoporous material derived from paper mill sludge and municipal sewage sludge for the effective degradation of organic pollutants.

Acknowledgments

The authors thank Dr. Xianjin Tang (Zhejiang University, China) for the preparation and characterization of samples. We would like to thank the National Natural Science Foundation (no. 20907045) of China and the Provincial Public Technology and Applied Research Projects by Science and Technology Department of Zhejiang Province (no. 2015C33049 and no. 2014C33020) for their financial support of this work.

References

[1] P. Hadi, M. Xu, C. Ning, C. Sze Ki Lin, G. McKay, A critical review on preparation, characterization and utilization of sludge-derived activated carbons for wastewater treatment, Chem. Eng. J., 260 (2015) 895–906.

[2] E.J. Scoton, R.A.G. Battistelle, B.S. Bezerra, J. Akutsu, A sewage sludge co-composting process using respirometric monitoring method in hermetic rotary reactor, J. Cleaner Prod., 121 (2016) 169–175.

[3] X. Dou, D. Chen, Y. Hu, Y. Feng, X. Dai, Carbonization of heavy metal impregnated sewage sludge oriented towards potential co-disposal, J. Hazard. Mater., 321 (2016) 132–145.

[4] Y. Tu, S. Tian, L. Kong, Y. Xiong, Co-catalytic effect of sewage sludge-derived char as the support of Fenton-like catalyst, Chem. Eng. J., 185–186 (2012) 44–51.

[5] A. Prince-Pike, D.I. Wilson, S. Baroutian, J. Andrews, D.J. Gapes, A kinetic model of municipal sludge degradation during non-catalytic wet oxidation, Water Res., 87 (2015) 225–236.

[6] R.R.N. Marques, F. Stüber, K.M. Smith, A. Fabregat, C. Bengoa, J. Font, A. Fortuny, S. Pullket, G.D. Fowler, N.J.D. Graham, Sewage sludge based catalysts for catalytic wet air oxidation of phenol: preparation characterisation and catalytic performance, Appl. Catal., B, 101 (2011) 306–316.

[7] S.J.T. Pollard, G.D. Fowler, C.J. Sollars, R. Perry, Low-cost adsorbents for waste and wastewater treatment a review, Sci. Total Environ., 116 (1992) 31–52.

[8] M.J. Martin, E. Serra, A. Ros, M.D. Balaguer, M. Rigola, Carbonaceous adsorbents from sewage sludge and their application in a combined activated sludge-powdered activated carbon (AS-PAC) treatment, Carbon, 42 (2004) 1389–1394.

[9] G. Wen, Z.H. Pan, J. Ma, Z.Q. Liu, L. Zhao, J.J. Li, Reuse of sewage sludge as a catalyst in ozonation – efficiency for the removal of oxalic acid and the control of bromate formation, J. Hazard. Mater., 239–240 (2012) 381–388.

[10] J.S. Cha, J.C. Choi, J.H. Ko, Y.K. Park, S.H. Park, K.E. Jeong, S.S. Kim, J.K. Jeon, The low-temperature SCR of NO over rice straw and sewage sludge derived char, Chem. Eng. J., 156 (2010) 321–327.

[11] X. Wang, B. Zhao, X. Yang, Co-pyrolysis of microalgae and sewage sludge: biocrude assessment and char yield prediction, Energy Convers. Manage., 117 (2016) 326–334.

[12] H. Chen, D. Chen, L. Hong, Influences of activation agent impregnated sewage sludge pyrolysis on emission characteristics of volatile combustion and De-NOx performance of activated char, Appl. Energy, 156 (2015) 767–775.

[13] J. Zhang, Q. Wang, Sustainable mechanisms of biochar derived from brewers' spent grain and sewage sludge for ammonia–nitrogen capture, J. Cleaner Prod., 112 (2016) 3927–3934.

[14] V.M. Monsalvo, A.F. Mohedano, J.J. Rodriguez, Activated carbons from sewage sludge: application to aqueous-phase adsorption of 4-chlorophenol, Desalination, 277 (2011) 377–382.

[15] A.N. Soon, B.H. Hameed, Heterogeneous catalytic treatment of synthetic dyes in aqueous media using Fenton and photo-assisted Fenton process, Desalination, 269 (2011) 1–16.

[16] W. Zhang, J. Zheng, P. Zheng, R. Qiu, Atrazine immobilization on sludge derived biochar and the interactive influence of coexisting Pb(II) or Cr(VI) ions, Chemosphere, 134 (2015) 438–445.

[17] Y. Tu, Y. Xiong, S. Tian, L. Kong, C. Descorme, Catalytic wet air oxidation of 2-chlorophenol over sewage sludge-derived carbon-based catalysts, J. Hazard. Mater., 276 (2014) 88–96.

[18] A. Bagreev, T.J. Bandosz, H_2S adsorption/oxidation on materials obtained using sulfuric acid activation of sewage sludge-derived fertilizer, J. Colloid Interface Sci., 252 (2002) 188–194.

[19] L. Gu, N. Zhu, P. Zhou, Preparation of sludge derived magnetic porous carbon and their application in Fenton-like degradation of 1-diazo-2-naphthol-4-sulfonic acid, Bioresour. Technol., 118 (2012) 638–642.

[20] S.J. Yuan, X.H. Dai, Facile synthesis of sewage sludge-derived mesoporous material as an efficient and stable heterogeneous catalyst for photo-Fenton reaction, Appl. Catal., B, 154–155 (2014) 252–258.

[21] H. Liu, L.L. Yi, Q. Zhang, H. Hu, G. Lu, A. Li, H. Yao, Co-production of clean syngas and ash adsorbent during sewage sludge gasification: synergistic effect of Fenton peroxidation and CaO conditioning, Appl. Energy, 179 (2016) 1062–1068.

[22] M.R. Carrasco-Díaz, E. Castillejos-López, A. Cerpa-Naranjo, M.L. Rojas-Cervantes, Efficient removal of paracetamol using $LaCu_{1-x}M_xO_3$ (M = Mn, Ti) perovskites as heterogeneous Fenton-like catalysts, Chem. Eng. J., 304 (2016) 408–418.

[23] K.A. Sashkina, A.V. Polukhin, V.S. Labko, A.B. Ayupov, A.I. Lysikov, E.V. Parkhomchuk, Fe-silicalites as heterogeneous Fenton-type catalysts for radiocobalt removal from EDTA chelates, Appl. Catal., B, 185 (2016) 353–361.

[24] L. Kong, Y. Xiong, L. Sun, S. Tian, X. Xu, C. Zhao, R. Luo, X. Yang, K. Shih, H. Liu, Sorption performance and mechanism of a sludge-derived char as porous carbon-based hybrid adsorbent for benzene derivatives in aqueous solution, J. Hazard. Mater., 274 (2014) 205–211.

[25] G. Zhou, Z. Chen, F. Fang, Y. He, H. Sun, H.X. Shi, Fenton-like degradation of Methylene Blue using paper mill sludge-derived magnetically separable heterogeneous catalyst: characterization and mechanism, J. Environ. Sci., 35 (2015) 20–26.

[26] G. Zhou, F. Fang, Z. Chen, Y. He, H. Sun, H.X. Shi, Facile synthesis of paper mill sludge-derived heterogeneous catalyst for the Fenton-like degradation of methylene blue, Catal. Commun., 62 (2015) 71–74.

[27] S. Garcia-Segura, J.A. Garrido, R.M. Rodriguez, P.L. Cabot, F. Centellas, C. Arias, E. Brillas, Mineralization of flumequine in acidic medium by electro-Fenton and photoelectro-Fenton processes, Water Res., 46 (2012) 2067–2076.

[28] S. Karthikeyan, A. Titus, A. Gnanamani, A.B. Mandal, G. Sekaran, Treatment of textile wastewater by homogeneous and heterogeneous Fenton oxidation processes, Desalination, 281 (2011) 438–445.

[29] H. Hassan, B.H. Hameed, Oxidative decolorization of Acid Red 1 solutions by Fe–zeolite Y type catalyst, Desalination, 276 (2011) 45–52.

[30] B.A. Ünnü, G. Gündüz, M. Dükkancı, Heterogeneous Fenton-like oxidation of crystal violet using an iron loaded ZSM-5 zeolite, Desal. Wat. Treat., 57 (2015) 11835–11849.

[31] Y. Wang, Y. Chen, J. Wang, J. Lu, Resin-supported Fe(III) as an efficient heterogeneous Fenton catalyst for degradation of Reactive Black 5, Desal. Wat. Treat., 57 (2015) 22039–22048.

[32] F. Chen, S. Xie, X. Huang, X. Qiu, Ionothermal synthesis of Fe_3O_4 magnetic nanoparticles as efficient heterogeneous Fenton-like catalysts for degradation of organic pollutants with H_2O_2, J. Hazard. Mater., 322 (2017) 152–162.
[33] M.B. Kasiri, H. Aleboyeh, A. Aleboyeh, Degradation of Acid Blue 74 using Fe-ZSM5 zeolite as a heterogeneous photo-Fenton catalyst, Appl. Catal., B, 84 (2008) 9–15.
[34] J. Sheng-tao, Z. Jian-zhong, B. Shu-li, G. Yu-jiang, Y. Jun, Research on Fe-loaded ZSM-5 molecular sieve catalyst in high-concentration aniline wastewater treatment, Desal. Wat. Treat., 57 (2016) 791–798.
[35] Q.H. Lin, H. Cheng, G.Y. Chen, Preparation and characterization of carbonaceous adsorbents from sewage sludge using a pilot-scale microwave heating equipment, J. Anal. Appl. Pyrolysis, 93 (2012) 113–119.
[36] Q. Wen, C. Li, Z. Cai, W. Zhang, H. Gao, L. Chen, G. Zeng, X. Shu, Y. Zhao, Study on activated carbon derived from sewage sludge for adsorption of gaseous formaldehyde, Bioresour. Technol., 102 (2011) 942–947.
[37] H. Fan, K. He, J. Wang, Study of sewage sludge pyrolysis liquids using comprehensive two-dimensional gas chromatography/time-of-flight mass spectrometry, Fuel, 185 (2016) 281–288.
[38] J. Du, J. Bao, X. Fu, C. Lu, S.H. Kim, Facile preparation of S/Fe composites as an effective peroxydisulfate activator for RhB degradation, Sep. Purif. Technol., 163 (2016) 145–152.
[39] L. Zhang, Y. He, Y. Wu, T. Wu, Photocatalytic degradation of RhB over $MgFe_2O_4/TiO_2$ composite materials, Mater. Sci. Eng., B, 176 (2011) 1497–1504.
[40] L.C.A. Oliveira, C.N. Silva, M.I. Yoshida, R.M. Lago, The effect of H_2 treatment on the activity of activated carbon for the oxidation of organic contaminants in water and the H_2O_2 decomposition, Carbon, 42 (2004) 2279–2284.
[41] A.R. Yeddou, B. Nadjemi, F. Halet, A. Ould-Dris, R. Capart, Removal of cyanide in aqueous solution by oxidation with hydrogen peroxide in presence of activated carbon prepared from olive stones, Miner. Eng., 23 (2010) 32–39.
[42] T. Wang, G. Qu, S. Pei, D. Liang, S. Hu, Research on dye wastewater decoloration by pulse discharge plasma combined with charcoal derived from spent tea leaves, Environ. Sci. Pollut. Res. Int., 23 (2016) 13448–13457.
[43] S. Guo, N. Yuan, G. Zhang, J.C. Yu, Graphene modified iron sludge derived from homogeneous Fenton process as an efficient heterogeneous Fenton catalyst for degradation of organic pollutants, Microporous Mesoporous Mater., 238 (2017) 62–68.